This is a repository copy of *Solid-state processing of surplus aluminium alloy powders through a combination of field-assisted sintering technology and hot rolling*.

White Rose Research Online URL for this paper:
https://eprints.whiterose.ac.uk/199543/

Version: Published Version

Article:
Graham, S.J. orcid.org/0000-0002-1296-1680, Patel, A., Fernandez Silva, B. et al. (4 more authors) (2023) Solid-state processing of surplus aluminium alloy powders through a combination of field-assisted sintering technology and hot rolling. Powder Metallurgy, 66 (3). pp. 187-194. ISSN 0032-5899

https://doi.org/10.1080/00325899.2023.2171582

Reuse
This article is distributed under the terms of the Creative Commons Attribution (CC BY) licence. This licence allows you to distribute, remix, tweak, and build upon the work, even commercially, as long as you credit the authors for the original work. More information and the full terms of the licence here: https://creativecommons.org/licenses/

Takedown
If you consider content in White Rose Research Online to be in breach of UK law, please notify us by emailing eprints@whiterose.ac.uk including the URL of the record and the reason for the withdrawal request.

eprints@whiterose.ac.uk
https://eprints.whiterose.ac.uk/

Check for updates

POWDER METALLURGY
2023, VOL. 66, NO. 3, 187–194
https://doi.org/10.1080/00325899.2023.2171582

I·M3 Institute of Materials, Minerals & Mining

Taylor & Francis
Taylor & Francis Group

OPEN ACCESS Check for updates

Solid-state processing of surplus aluminium alloy powders through a combination of field-assisted sintering technology and hot rolling

S. J. Graham [a], A. Patel[a], B. Fernandez Silva[a], W. Stott[b], G. J. Baxter[a], M. Roscher[c] and M. Jackson[a]

[a]Department of Materials Science and Engineering, The University of Sheffield, Sheffield, UK; [b]Aluminium Materials Technologies Ltd, Worcester, UK; [c]ECKART GmbH, Hartenstein, Germany

ABSTRACT

Metal additive manufacturing techniques typically operate using powders with limited particle size ranges, but atomisation processes produce significant amounts of particles outside these ranges, resulting in an accumulation of out-of-size specification metal powders without a clear use case. Field-assisted sintering technology (FAST) can provide an alternative, solid-state processing route to consolidate these powders into billets for subsequent processing, or directly into near-net shape components. In this study, surplus powders of A20X, an aerospace approved aluminium alloy developed by Aluminium Materials Technologies (ECKART GmbH), were processed using FAST and subsequently hot rolled to produce sheet material. Tensile properties were similar to hot rolled conventional cast material and comparable to additively manufactured product. This indicates that FAST is an effective option for converting surplus metal powders into useful products, while improving sustainability in the additive supply chain.

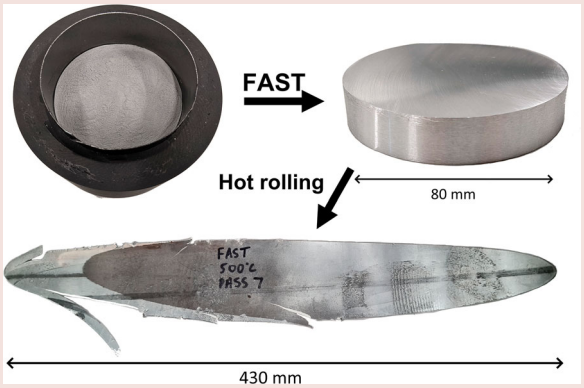

ARTICLE HISTORY
Received 24 October 2022
Revised 16 January 2023
Accepted 18 January 2023

KEYWORDS
Field-assisted sintering technology; spark plasma sintering; aluminium alloy; hot rolling; solid-state processing; microstructural evolution; tensile properties

Introduction

Interest from both industry and academia in additive manufacturing (AM) continues to grow, and the production of parts via AM technologies provides exciting opportunities in many new and existing applications. Consequently, the wider use of powder-based metal AM will need increased quantities of atomised metal powders to be produced. Unfortunately, there is limited control over the particle size distribution (PSD) obtained through atomisation, resulting in wider than desirable particle size ranges. Each AM technique has requirements for both particle morphology and size and, although a combination of AM and other powder metallurgy techniques can be used, it is generally the case that individual atomisation runs are done with a specific alloy and technique in mind [1]. Re-melting of surplus powder is possible for some alloy systems, but not viable for aluminium and titanium alloys as significant oxygen pickup can adversely affect final mechanical properties. This is leading to an accumulation of unsaleable, surplus powders, with no clear end-use.

A20X is a high-strength aluminium alloy with high-temperature capability, patented and manufactured by ECKART GmbH (Table 1). It is used in both a cast form and, more recently, in powder form for metal AM to produce complex and lightweight components for the aerospace, defence and automotive sectors [2]. A20X powder is produced by gas atomisation (GA) and supplied for use in

CONTACT S. J. Graham s.j.graham@sheffield.ac.uk Department of Materials Science and Engineering, The University of Sheffield, Sir Robert Hadfield Building, Mappin Street, Sheffield, S1 3JD, UK

© 2023 The Author(s). Published by Informa UK Limited, trading as Taylor & Francis Group
This is an Open Access article distributed under the terms of the Creative Commons Attribution License (http://creativecommons.org/licenses/by/4.0/), which permits unrestricted use, distribution, and reproduction in any medium, provided the original work is properly cited. The terms on which this article has been published allow the posting of the Accepted Manuscript in a repository by the author(s) or with their consent.

Table 1. Chemical composition of the A20X aluminium alloy.

Element	Al	Cu	Mg	Ag	Ti	B	Si	Fe
wt-%	Bal.	4.2–5.0	0.20–0.33	0.60–0.90	3.0–3.9	1.3–1.6	0.10 max	0.080 max

laser powder bed fusion (LPBF) with a particle size range of 20–63 µm, for optimal powder flowability and spreadability. Particles below this range easily agglomerate, preventing them being properly deposited, whereas coarse particles cause the powder layers to be thicker, requiring a larger focal spot and reducing accuracy in the build [3]. Although there are many factors affecting the PSD achieved by GA, the yield of powder particles with diameters 20–63 µm is often 50% or less [4,5]. Given that the main application of A20X and comparable aluminium-based spherical powders is LPBF, excess powder of <20 µm and >63 µm size fractions is generated. This material is still high quality however and could be used to create products using other processing methods. Business economics require that alternative processes are utilised to convert these surplus powders into useful products, to ensure that the AM market is cost effective and meets sustainability targets.

Field-assisted sintering technology (FAST, also known as spark plasma sintering) is an effective consolidation technique for a wide variety of powder materials [6]. This includes aluminium alloys, for which FAST has an advantage over other consolidation techniques as the applied electrical current breaks the surface oxide layers on the powder particles, allowing them to fuse together far more effectively [7]. The high heating rates and applied pressure also lead to relatively short processing times, resulting in fine-grained microstructures. Although FAST is more limited than AM with respect to the complexity of near-net shape geometries which can be produced, it can be used as an intermediate solid-state step and combined with more conventional processes, such as forging [8,9]. A previous study has also demonstrated that hot rolling can significantly improve the mechanical properties of pure aluminium compacts made from powder using FAST [10]. In this research, the rolling behaviour of FAST processed A20X billets was investigated for the first time and compared to cast material. The ability to create high-strength sheet products from surplus powders in two steps is an attractive option, which could have many industrial applications.

Materials and methods

Fine and coarse fractions of A20X powder (<20 µm and 63–150 µm) were provided by ECKART GmbH. The powders were weighed and blended to give a mixture composed of 20 wt-% fine and 80 wt-% coarse, to demonstrate that both surplus fractions resulting from GA could be processed together via FAST. The PSD of the powder blend was measured by laser diffraction using a Malvern Mastersizer 3000, with an average of 10 measurements taken.

In total, 220 g of the powder blend was placed into an 80 mm internal diameter graphite ring mould lined with graphite foil for easy sample removal. An FCT Systeme GmbH type HP D 25 furnace was used for FAST processing, with the temperature measured by an optical pyrometer focussed on a location 5 mm away from the surface of the sample, made possible through a hole machined in the graphite tooling. Processing was done under vacuum and parameters included a maximum temperature of 500°C, 35 MPa pressure, with a dwell time of 30 min under these conditions. After cooling, the resulting 80 mm diameter, 15 mm thick billet was removed from the tooling. The surfaces of the billet were lightly ground using SiC grit paper to remove any residual graphite foil and rough edges.

A set of three 4 mm diameter round tensile bars (with dimensions specified in ASTM B557M) were machined from both the FAST processed billet and as-cast A20X alloy material taken from test bars from an investment casting. Additional investment cast material was machined to the same dimensions as the FAST billet for subsequent rolling and comparison. Tensile testing was performed at a constant crosshead speed of 0.6 mm min^{-1} using a ZwickRoell Z050 testing machine, equipped with a 50 kN load cell and a camera extensometer.

Prior to rolling, both the 80 mm diameter FAST and cast billets underwent a homogenisation heat treatment and were then pre-heated in a furnace at 500°C for 120 min prior to hot rolling. Rolling trails were carried out on a Fenn LLC - Model 081 reversible rolling mill, using a constant rolling speed of 2 m min^{-1}. The thickness of the billets was reduced from 15 to 2 mm after a total of seven passes. The intermediate rolled product was placed back into the furnace for 15 min after every other pass, down to 4.5 mm, then after each of the two remaining passes down to 2 mm. Two 2 mm thick sheets were produced, one from the FAST billet and one from the cast billet. Half of each underwent a T7 heat treatment to increase the strength, consisting of a two-step solution treatment (2 h at 505°C, followed by 4 h at 530°C), quenching in a 25% glycol/water solution, and aging at 190°C for 4 h.

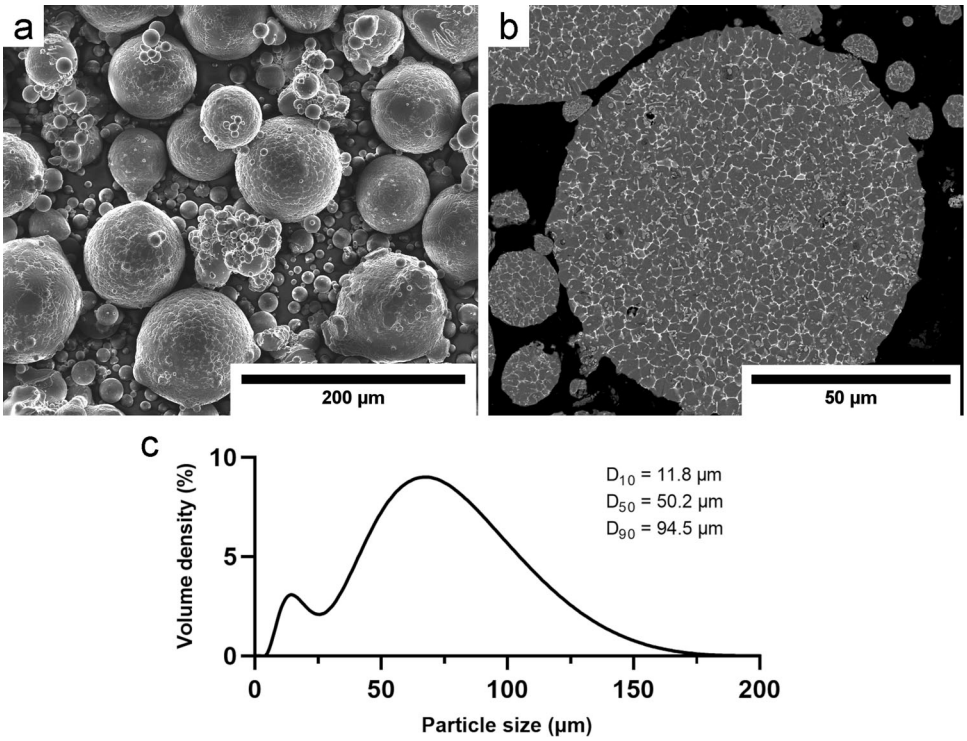

Figure 1. (a) Secondary electron micrograph of A20X powder blend and (b) backscattered electron micrograph of ground and polished A20X powder, bottom: PSD of A20X powder blend.

Sets of 6 mm wide flat tensile specimens (with dimensions specified in ASTM B557M) were extracted from the resulting sheets at 0°, 45° and 90° to the rolling direction (RD). Tensile testing was performed as described previously.

Samples were taken at each stage for microstructural analysis, including the powder blend, FAST processed billet, cast billet, as-rolled sheets and T7 heat-treated sheets. Sheet samples were sectioned to expose a cross-sectional area with dimensions in the RD and normal direction. SiC grit papers (P800-P2500) and colloidal silica were used to grind and polish the samples. Analysis was performed by scanning electron microscopy (SEM), using an FEI Inspect F50 microscope with an Oxford Instruments attachment for elemental analysis by energy-dispersive X-ray spectroscopy (X-EDS).

Texture analysis of the heat-treated sheet samples was performed by electron backscattered diffraction in a JEOL JSM-7900F SEM, equipped with a symmetry detector, using an accelerating voltage of 20 kV. The orientation mapping was undertaken using the AZtecHKL software for data collection covering areas of 300×230 µm^2 using a 0.5-µm step size to obtain orientation data for texture and grain size analysis. Only the α-Al phase was indexed. Further, post-processing was performed using Channel 5 to clean up the dataset, removing black pixels caused by the unindexed TiB_2 phase to give a clearer view of the α-Al grains. MTEX was then used to plot the orientation maps and pole figures.

Results and discussion

A20X powder analysis

Figure 1 shows the spherical morphology of the A20X powder particles, resulting from the GA process. The smaller particles tended to agglomerate, whereas the larger particles remained discrete. These agglomerations were on a similar scale to individual particles of the coarse powder, and therefore caused no issues during blending or loading of the graphite ring mould. The cross-section of the particles in Figure 1 revealed the fine-grained microstructure generated by rapid solidification and from grain refinement provided by the TiB_2 addition in this alloy. Analysis of the PSD showed two peaks at around 15 and 70 µm, corresponding to the undersize and oversize fractions, respectively. There was some overlap between the two powder sizes and the conventionally supplied 20–63 µm range, due to limitations of the sieving process.

Analysis of FAST processed and cast A20X

The micrograph of the cast A20X in Figure 2(a) showed relatively large α-Al grains, with coarse Al_2Cu intermetallic precipitates concentrated at the grain boundaries, which act as nucleation sites for precipitation. The difference in cast microstructure from atomised powder was due to the much slower cooling rate experienced. TiB_2 ceramic particles

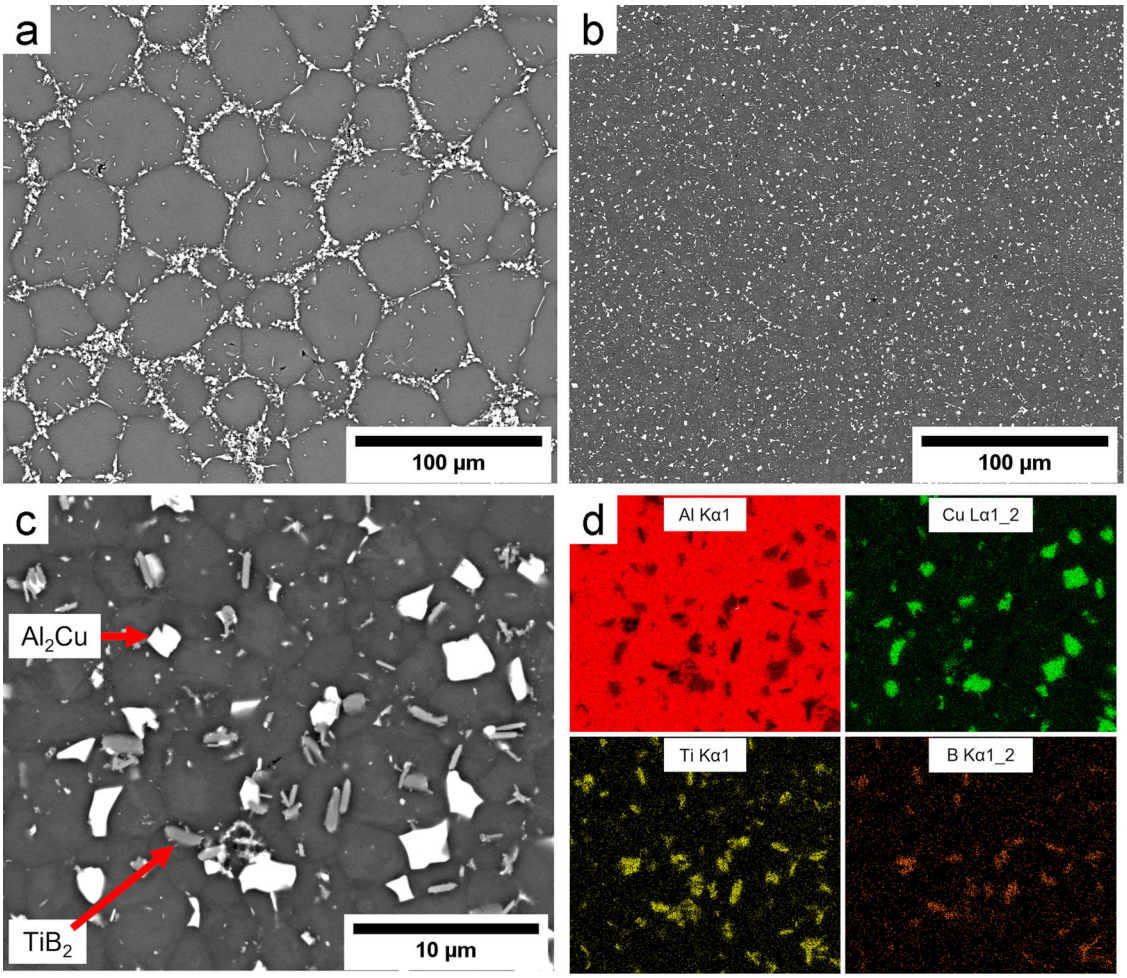

Figure 2. (a) Backscattered electron micrograph of as-cast A20X alloy, (b&c) backscattered electron micrographs of FAST processed A20X powders and (d) X-EDS element maps corresponding to the micrograph in c.

were also localised at the grain boundaries, due to being pushed there during solidification. In contrast, much finer grains were present in the FAST processed material, with the Al_2Cu and TiB_2 phases evenly dispersed (Figures 2(b and c)). Retention of the fine-grained microstructure from the powder particles shown in Figure 1 highlights how the solid-state FAST process efficiently consolidated the powder to full density, without causing significant grain growth. The 30 min dwell time at 500°C caused most of the copper dissolved into the α phase, and cooling occurred relatively slowly due to processing under vacuum and use of thermal insulation, causing some re-precipitation and growth of large intermetallic

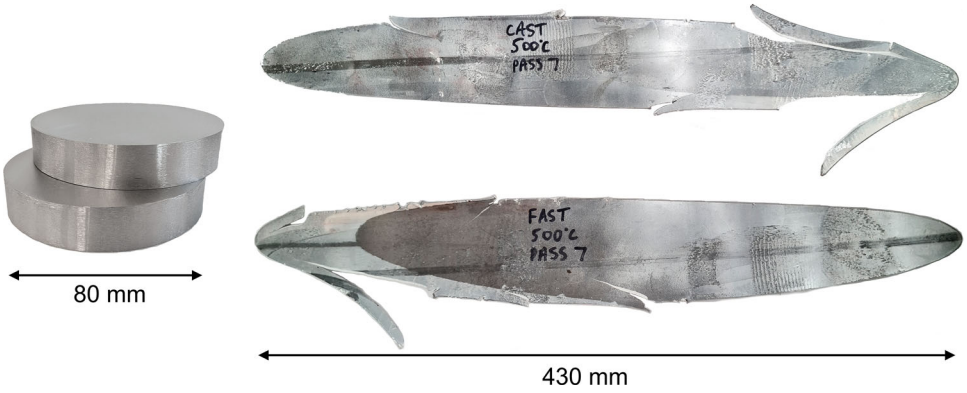

Figure 3. Left: photograph of 80 mm diameter FAST processed and cast billets, right: 2 mm thick sheets after hot rolling. Top sheet derived from cast billet, bottom sheet derived from FAST processed billet.

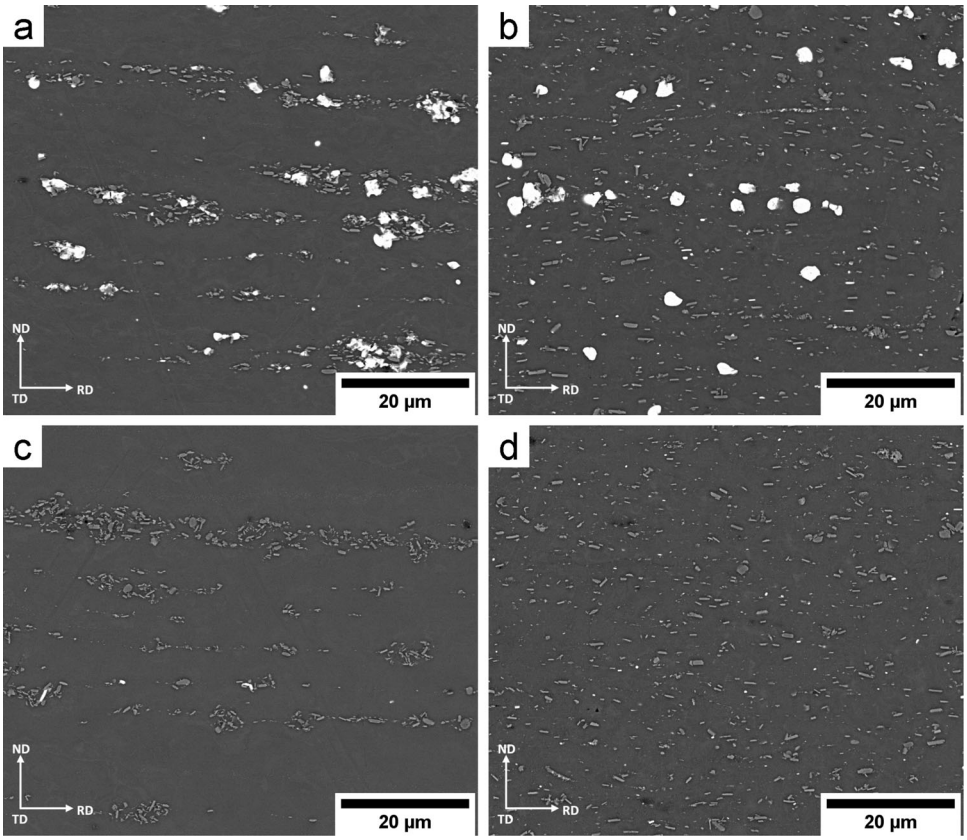

Figure 4. Backscattered electron micrographs of (a) as-rolled cast sheet, (b) as-rolled FAST processed sheet, (c) rolled and heat-treated cast sheet and (d) rolled and heat-treated FAST processed sheet. RD – rolling direction, ND – normal direction, TD – transverse direction.

Al_2Cu, which was on a similar scale to the α grains. X-EDS point analysis confirmed the composition of the different phases present, with major alloying element maps in Figure 2(d) showing the even distribution of these phases in the FAST processed material. Silver and magnesium have low solubilities in the α phase at room temperature and were not concentrated anywhere in the X-EDS maps, so were likely present in fine intermetallic phases.

Hot rolling behaviour and microstructural analysis of A20X sheets

Both the cast and FAST processed billets were successfully hot rolled from their initial 15 mm thickness down to 2 mm. They behaved similarly during hot rolling, with small amounts of edge cracking and peeling present by the final pass, as shown in Figure 3. The quality of the sheets resulting from this initial trial could be improved upon through optimisation of the various parameters, including soaking temperature, rolling speed, reduction per passes, frequency of re-heating and use of heated rolls. Owing to the small starting size of the billets, they tended to lose heat faster when in contact with the rolls, meaning that the material could be significantly cooler during the reverse passes. This resulted in more work hardening and a greater force required on each reverse pass. Unfortunately, the rolling load and temperature were not able to be measured at the time to quantify this effect.

Specimens were extracted from the sheet material for metallography and tensile testing, before and after the T7 heat treatment. The micrographs in Figure 4 highlight how the rolling process caused distinct changes in the microstructure of both materials. In the as-rolled condition, the Al_2Cu phase was present in both with similar size and morphology to those seen in Figure 2(c), suggesting it was unaffected by the rolling process. This was likely because at the hot rolling temperature of 500°C, most of the copper dissolved into the α phase, and remained so during rolling. Slow cooling then caused re-precipitation of coarse Al_2Cu particles. In contrast, the TiB_2 particles were present throughout and became aligned in the RD. The TiB_2 in the cast sheet appeared in distinct bands, whereas the particles were evenly distributed in the FAST sheet. This corresponds with the microstructure shown in Figure 2(a), suggesting that the 'rings' of TiB_2 which previously bordered the large, equiaxed cast grains were also elongated in the RD.

The micrographs of the T7 heat-treated sheets in Figure 4 were essentially identical to those of the as-rolled condition, but without the Al_2Cu precipitates. First, the solution treatment caused the copper to dissolve into the α phase, where it was retained in a solid

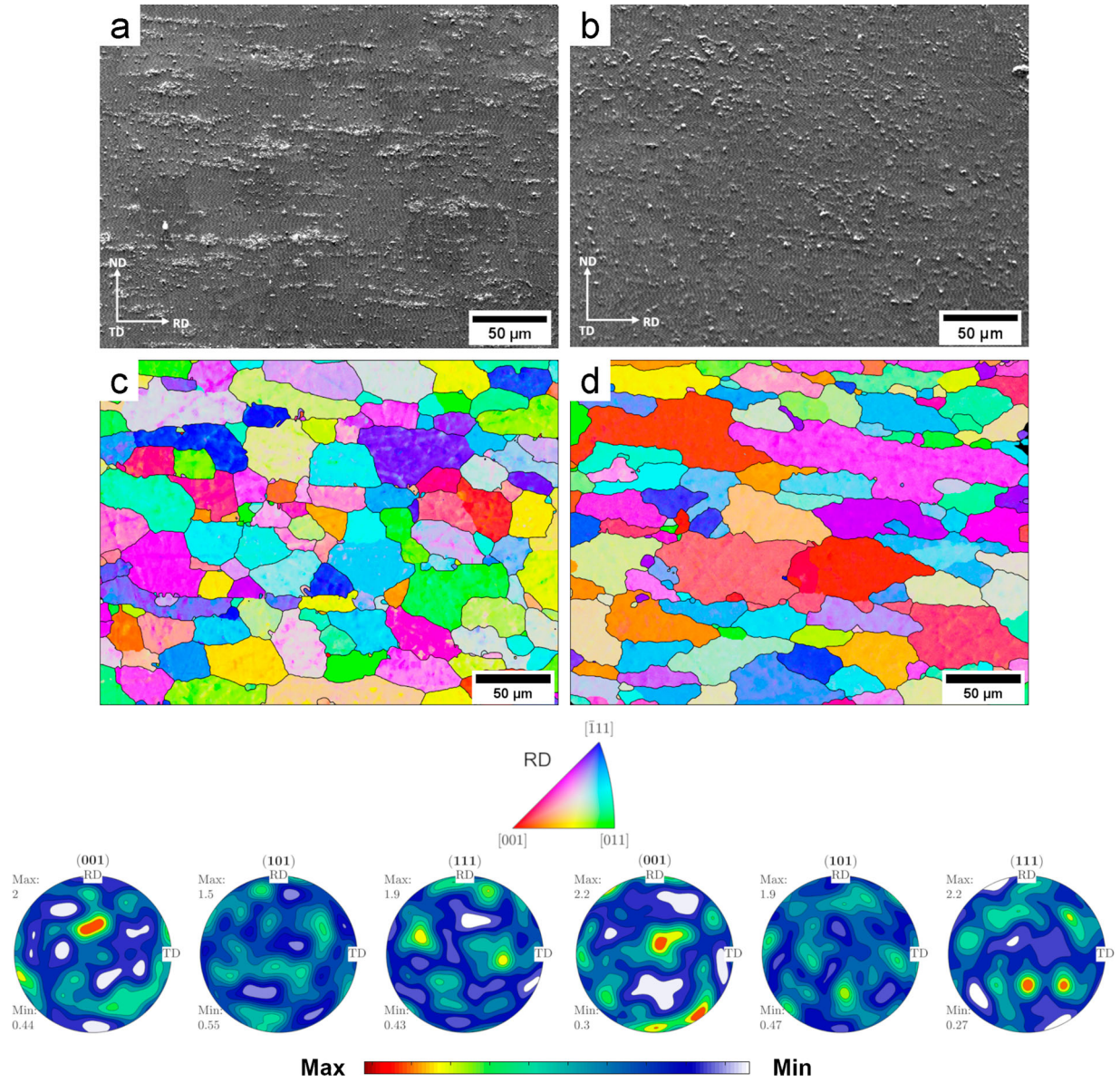

Figure 5. Forward scattered electron micrographs and inverse pole figure orientation maps with respect to the RD of sheet product after T7 heat treatment derived from cast (a&c) and FAST processed (b&d) material. Corresponding pole figure plots are shown below.

solution on quenching. Aging then caused the copper to re-precipitate as Al_2Cu, although this was controlled and occurred slowly, resulting in extremely fine particles that were not detectable at the magnification used in SEM. The morphology and distribution of the TiB_2 remained unaffected by the T7 heat treatment. The texture analysis in Figure 5 revealed the α grain structure of the T7 heat-treated sheets. Recrystallisation caused the grain size to approximately equalise between both materials, with much larger grains present in the FAST sheet compared to directly after powder consolidation. It was more pronounced in the lower magnification micrographs in Figure 5(a and b) how the TiB_2 particles were more evenly distributed in the solid-state FAST-derived sheet compared to cast. Both samples showed random and weak texture, with no preferred orientation towards a particular direction. The FAST sample consisted of grains elongated in the RD while the cast sample had a more uniform and equiaxed microstructure, although it is unclear exactly what caused this difference between them. Given that both billets experienced the same thermomechanical processing, any variation in properties must result from the different starting materials, with more in-depth analysis required to fully understand the microstructural evolution during this processing route.

Comparing the tensile properties of FAST processed and cast A20X at each processing stage

Figure 6 and Table 2 present the tensile behaviour of both cast and FAST processed A20X alloy, and how it changed after hot rolling and the following T7 heat treatment. Although both the cast and FAST

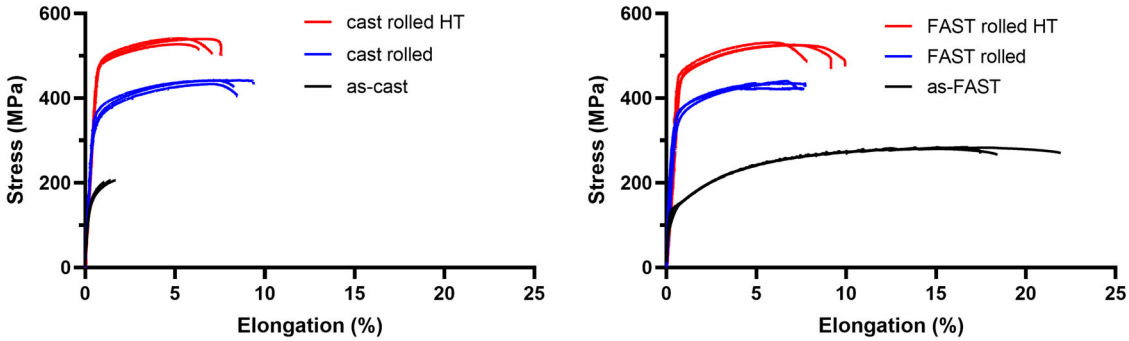

Figure 6. Stress/elongation curves comparing the behaviour of cast and FAST processed A20X material, before rolling, in the as-rolled condition and after T7 heat treatment (HT).

Table 2. Mechanical property data obtained from tensile testing. AM results used from Ref. [11].

Sample	Specimen angle relative to RD	0.2% yield strength (MPa)	Ultimate tensile strength (MPa)	Elongation at break (%)
As-cast (mean average values)	N/A	173	206	1.4
As-FAST (mean average values)	N/A	151	284	19
Cast rolled	0°	364	442	8.3
	45°	338	442	8.5
	90°	341	433	9.4
FAST rolled	0°	368	432	7.7
	45°	341	440	7.3
	90°	344	435	7.7
Cast rolled T7 HT	0°	481	540	7.6
	45°	487	541	7.1
	90°	469	527	6.4
FAST rolled T7 HT	0°	462	531	7.8
	45°	455	525	9.9
	90°	457	526	9.2
AM-LPBF as-built	(Orthogonal to build direction)	360	429	14
AM-LPBF T6 HT		428	486	14

processed material have similar yield strengths, the latter exhibited far greater ductility. This can be attributed to the more homogeneous microstructure and even dispersion of Al_2Cu and TiB_2 phases. Al_2Cu is a brittle intermetallic phase, and so the large clusters in Figure 2(a) function as crack propagation sites, which are detrimental to ductility. Although a much finer grain microstructure is present in FAST processed material, this did not translate to a higher strength, which would be expected based on the Hall-Petch relationship. This implies that grain size is not the primary factor in the strength of this alloy, but instead precipitation and dispersion hardening from the intermetallic phases and TiB_2, respectively.

The strength of both materials increased significantly after rolling, and even further post T7 heat treatment, with both exhibiting similar properties. The hot rolling and T7 heat treatment altered the microstructures such that the materials behaved similarly under tensile loading, in contrast to the materials prior to rolling. The differing dispersion of TiB_2 must not have had a significant effect on tensile properties, as this was the major difference between the two rolled microstructures. The additional increase in strength achieved by the T7 heat treatment was due to a combination of solid solution strengthening and precipitation strengthening from the presence of much finer Al_2Cu precipitates generated by aging, which impede dislocation movement.

Although each rolled tensile specimen was extracted at a different orientation (0°, 45° and 90°) relative to the RD, there was no considerable variation in the tensile properties, aside from slightly higher yield strength in the as-rolled 0° specimens. The yield strengths were more consistent after heat treatment though, indicating the final materials were isotropic. This also corresponds with the texture analysis as there was no preferential texture in either microstructure. The presence of more elongated grains in the heat-treated FAST sheet (shown in Figure 5) seemed to cause no directional effects on the mechanical properties compared to the corresponding cast sample. Further analysis and testing of more specimens would be required to confirm the consistency of these results, however.

The tensile properties were comparable with the data from literature values of AM-LPBF-produced material in Table 2 [11]. The strength of the as-rolled sheets was very similar to as-built material, but greater strength was achieved in the rolled product after T7 heat treatment, although the heat treatment used on the printed material was slightly different. The AM material was more ductile than the sheet materials, both before and after heat treatment, likely a

consequence of the finer microstructure achieved when processing this alloy by LPBF.

Conclusions

FAST has proven to be an effective technology for the consolidation of surplus A20X alloy powders, producing fully dense billets in a short processing time. By combining FAST with hot rolling, these powders were converted into sheet product, although some optimisation of the rolling process is required to prevent tearing. Larger starting billets could also mitigate edge effects and reduce heat loss during rolling. Comparison with conventional cast A20X material throughout processing highlighted the differences in microstructures obtained, with the FAST processed material possessing a more homogeneous dispersion of TiB_2 ceramic particles at every stage. Despite a large variation in the ductility of as-cast and as-FAST material, the hot rolling and subsequent heat treatment caused the two materials to perform similarly under tensile load. This demonstrates that the FAST processed powder performs well and can be considered an equal alternative material to conventional as-cast material. Although there was no obvious effect on tensile properties from the difference in the distribution of TiB_2 between cast and FAST sheets, it may affect other mechanical properties, such as fatigue and high temperature performance. Further testing is required, but the homogeneous microstructures obtained from FAST consolidated powder may perform better under cyclic loading. The tensile properties of the FAST sheet material were also comparable to data in the literature of more conventional LPBF printed A20X powder, demonstrating that this solid-state processing route can be used to produce competitive, high-performance material. The T7 heat-treated FAST sheet also exhibited tensile properties similar to conventional 2xxx and 7xxx series aluminium alloys currently used in aircraft fuselage and wing skins, highlighting its potential for application in the aerospace industry [12].

Acknowledgements

The authors also wish to thank Mike Bond, formerly of Aluminium Materials Technologies and ECKART GmbH, for initiating the project and collaboration; Aeromet International Ltd for providing the as-cast material, machining of tensile specimens, testing of the as-cast and as-FAST material and performing the T7 heat treatment; and technical staff at The University of Sheffield for assisting with the rolling trials: Neil Hind, Thomas Peace, Dr. Yunus Azakli, Nigel Adams, Richard Pears and Dr. Lisa Hollands.

Disclosure statement

No potential conflict of interest was reported by the author(s).

Funding

This work was supported by the Engineering and Physical Sciences Research Council (EPSRC) [grant number EP/P006566/1: 'MAPP: EPSRC Future Manufacturing Hub in Manufacture using Advanced Powder Processes'] and [grant number EP/R00661X/1: 'Sir Henry Royce Institute'].

ORCID

S. J. Graham http://orcid.org/0000-0002-1296-1680

References

[1] Moghimian P, Poirié T, Habibnejad-Korayem M, et al. Metal powders in additive manufacturing: a review on reusability and recyclability of common titanium, nickel and aluminum alloys. Addit Manuf. 2021;43:102017.
[2] A20X Technical Information Sheet [Internet]. ECKART GmbH; 2020 [cited 2022 Apr 24]. Available from: www.a20x.com.
[3] Yadroitsev I, Yadroitsava I, Du Plessis A. Basics of laser powder bed fusion. In: Yadroitsev I, editor. Fundamentals of laser powder Bed fusion of metals. Amsterdam: Elsevier; 2021. p. 15–38.
[4] Drawin S, Deborde A, Thomas M, et al. Atomization of Ti-64 alloy using the EIGA process: comparison of the characteristics of powders produced in labscale and industrial-scale facilities. In: Villechaise P, Appolaire B, Castany P, et al., editors. MATEC web conference. Red Hook, NY: Curran Associates, Inc.; 2020;321:07013.
[5] Gao C. Characterization of spherical AlSi10Mg powder produced by double-nozzle gas atomization using different parameters. Trans Nonferrous Met Soc China. 2019;29(2):374–384.
[6] Weston NS, Thomas B, Jackson M. Processing metal powders via field assisted sintering technology (FAST): a critical review. Mater Sci Technol. 2019;35:1306–1328.
[7] Awotunde MA, Adegbenjo AO, Shongwe MB, et al. Spark plasma sintering of aluminium-based materials. In: Cavaliere P, editor. Spark plasma sintering of materials. Cham: Springer; 2019. p. 191–218.
[8] Pope J, Jackson M. FAST-forge of diffusion bonded dissimilar titanium alloys: a novel hybrid processing approach for next generation near-net shape components. Metals (Basel). 2019;9:654.
[9] Weston NS, Jackson M. FAST-forge – a new cost-effective hybrid processing route for consolidating titanium powder into near net shape forged components. J Mater Process Technol. 2017;243:335–346.
[10] Sadeghi B, Shabani A, Cavaliere P. Hot rolling of spark-plasma-sintered pure aluminium. Powder Metall. 2018;61:285–292.
[11] Belelli F. Investigation on two Ti–B-reinforced Al alloys for laser powder bed fusion. Mater Sci. 2021;808:140944.
[12] Dursun T, Soutis C. Recent developments in advanced aircraft aluminium alloys. Mater Des (1980-2015). 2014;56:862–871.